JACS
JOURNAL OF THE AMERICAN CHEMICAL SOCIETY
Cite This: J. Am. Chem. Soc. 2019, 141, 8698−8702
Communication
pubs.acs.org/JACS

Gas-Phase Photolysis of Hg(I) Radical Species: A New Atmospheric Mercury Reduction Process

Alfonso Saiz-Lopez,*[,†] A. Ulises Acuña,[†] Tarek Trabelsi,[‡] Javier Carmona-García,[§] Juan Z. Dávalos,[†] Daniel Rivero,[†] Carlos A. Cuevas,[†] Douglas E. Kinnison,[∥] Sebastian P. Sitkiewicz,[⊥] Daniel Roca-Sanjuán,*[,§] and Joseph S. Francisco*[,‡]

[†]Department of Atmospheric Chemistry and Climate, Institute of Physical Chemistry Rocasolano, CSIC, Madrid 28006, Spain
[‡]Department of Earth and Environmental Sciences and Department of Chemistry, University of Pennsylvania, Philadelphia, Pennsylvania 19104, United States
[§]Institut de Ciència Molecular, Universitat de València, Valencia 46071, Spain
[∥]Atmospheric Chemistry Observations and Modelling, NCAR, Boulder, Colorado 80301, United States
[⊥]Kimika Fakultatea, Euskal Herriko Unibertsitatea UPV/EHU and Donostia International Physics Center (DIPC), P.K. 1072, 20080 Donostia, Euskadi, Spain

Supporting Information

ABSTRACT: The efficient gas-phase photoreduction of Hg(II) has recently been shown to change mercury cycling significantly in the atmosphere and its deposition to the Earth's surface. However, the photolysis of key Hg(I) species within that cycle is currently not considered. Here we present ultraviolet−visible absorption spectra and cross-sections of HgCl, HgBr, HgI, and HgOH radicals, computed by high-level quantum-chemical methods, and show for the first time that gas-phase Hg(I) photoreduction can occur at time scales that eventually would influence the mercury chemistry in the atmosphere. These results provide new fundamental understanding of the photobehavior of Hg(I) radicals and show that the photolysis of HgBr increases atmospheric mercury lifetime, contributing to its global distribution in a significant way.

Mercury is a developmental neurotoxin that is transported in the atmosphere in elemental and oxidized forms. Elemental mercury is characterized by low chemical reactivity and it remains long enough in the atmosphere (6−12 months on average) to become a global contaminant, albeit in very low concentration ∼1−2 ng m^{-3}.

Anthropogenic emissions to the atmosphere are essentially in the elemental Hg(0) form which is oxidized to divalent Hg(II).[1,2] Its deposition to the surface environment and impact on ecosystems is greatly enhanced following Hg(0) oxidation to the divalent form, much more water-soluble and particle reactive and hence more prone to wet and dry deposition. Consequently, atmospheric Hg(II) reduction back to elemental mercury competes with surface deposition. Once deposited in rivers, lakes, and oceans, mercury is bioconverted to the extremely toxic methyl mercury, which is easily absorbed by living organisms and enriched through the trophic chain.[3]

It is currently assumed that Hg(0) atmospheric oxidation is initiated mainly via photochemically produced bromine (Br) atoms by a two-stage mechanism.[4,5] The first step yields an unstable intermediate, HgBr, which can thermally dissociate back to Hg(0) or be further oxidized to divalent mercury Hg(II) by secondary oxidants, such as OH, Br, I, Cl, NO_2, HO_2, BrO, IO, and ClO. Although HgCl, HgI, and HgOH radicals can also be produced, their formation rate is 3−4 times slower than that of the brominated monohalide.[3]

A recent study has shown that fast gaseous photoreduction of the resulting Hg(II) species can have a major impact on global atmospheric mercury dynamics and its deposition to the surface environment.[6] However, the photodissociation of the HgBr radical back to Hg(0), which would crucially determine its lifetime in the troposphere, has been overlooked in the current mechanism of atmospheric mercury chemistry.[1,4] In this Communication, we report detailed spectroscopic properties of HgX (X = Cl, Br, I, OH) species, computed by robust theoretical methods, which are critical to showing for the first time the importance of photodissociation of Hg(I) for the atmospheric mercury cycle.

Previous computational studies of mercury compounds have been recently reviewed[3,7−10] and were concerned mainly with ground-state properties of closed-shell compounds. In addition, a few theoretical studies addressed selected spectral properties of electronic excited-states of Hg(I) halide radicals such as the radiative lifetimes of the $B \rightarrow X$ transition,[11] the low-lying electronic states of HgCl and HgBr,[12] the $X-A$ transition in HgCl[13] and HgBr[14] and two low-lying electronic states of both species.[13−15]

Here we applied the state-averaged complete active space self-consistent field (CASSCF) method,[16,17] followed by multireference configuration interaction (MRCI)[18,19] including the Davidson correction (MRCI+Q),[20] to determine potential energy curves (PECs), geometrical (bond lengths and angles), and thermochemical (bond dissociation energies) properties of the HgX radicals. In addition, we also used multistate complete active space second-order perturbation theory, (MS-

Received: March 15, 2019
Published: May 22, 2019

DOI: 10.1021/jacs.9b02890
J. Am. Chem. Soc. 2019, 141, 8698−8702

CASPT2)[21−24] as implemented in MOLCAS,[25] to predict absorption spectra and cross-sections by well-established computational techniques,[26,27] used before for spectra calculation of a series of Hg(II) compounds.[6] Finally, a kinetic model for the atmospheric redox (photo)chemistry of the Hg(0), Hg(I), and Hg(II) species was built based on the computed data (see Supporting Information (SI)).

The relevant molecular orbitals of the HgX (X = Cl, Br, I, OH) radicals are shown in Figure 1, while Tables S1−S3

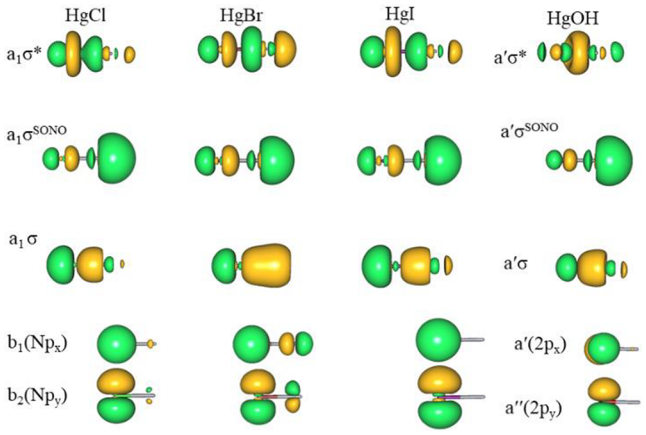

Figure 1. Natural orbitals (isovalue = 0.05) of HgX (X = Cl, Br, I, and OH).

present geometrical and thermochemical data calculated for these species, both in the ground and first bound electronically excited-state, together with previous available experimental and computed values.

The PEC diagrams of these radical species were calculated including spin-orbit (SO) coupling. Those corresponding to HgBr, as a function of the internuclear distance, and HgOH as a function of the Hg−OH coordinate are shown in Figure 2. The remaining PECs are displayed in Figures S1 and S2. The electronic-state nomenclature designated in previous spectroscopic analysis[28−30] is retained here. For the HgX (X = Cl, Br, I) monohalides, *A* and *B* denote the lowest-lying excited spin free (SF) states $^2\Pi$ and $^2\Sigma^+$ and *C* and *D* is used for each of the SO states (with Ω = 1/2 and 3/2) related to the high-energy $^2\Pi$ SF state. The ground and excited electronic states of all the HgX radicals computed here contain mixtures of ionic and covalent configurations, as was noted by previous calculations of the Cl and Br mercury monohalides.[12]

The calculated bond-dissociation energy (D_0) of the weakly bound $X\ ^2\Sigma^+$ ground-state of the monohalides (Tables S1 and S2) decreases rapidly from ≈100 (Cl) to ≈30 (I) kJ·mol^{-1}, in very good agreement with existing experimental data. The agreement extends also to equilibrium geometry and harmonic frequencies. In the case of the isoelectronic HgOH radical, the ground-state binding energy of the Hg−OH bond is even lower, and would compromise the stability of this radical. Inclusion of SO effects does not affect the D_0 values, since the electronic ground-state correlates to the lowest dissociation limit Hg (^{1}S) and X($^2P_{3/2}$). The first electronically excited-state ($A\ ^2\Pi$) of the halogenated radicals (Figure 2a and Figure S1), which is the most relevant for the present work, is strictly repulsive as noted in previous calculations of Wadt.[12]

The repulsive character of this state, which has received little attention, can be interpreted based on two factors: (i) a

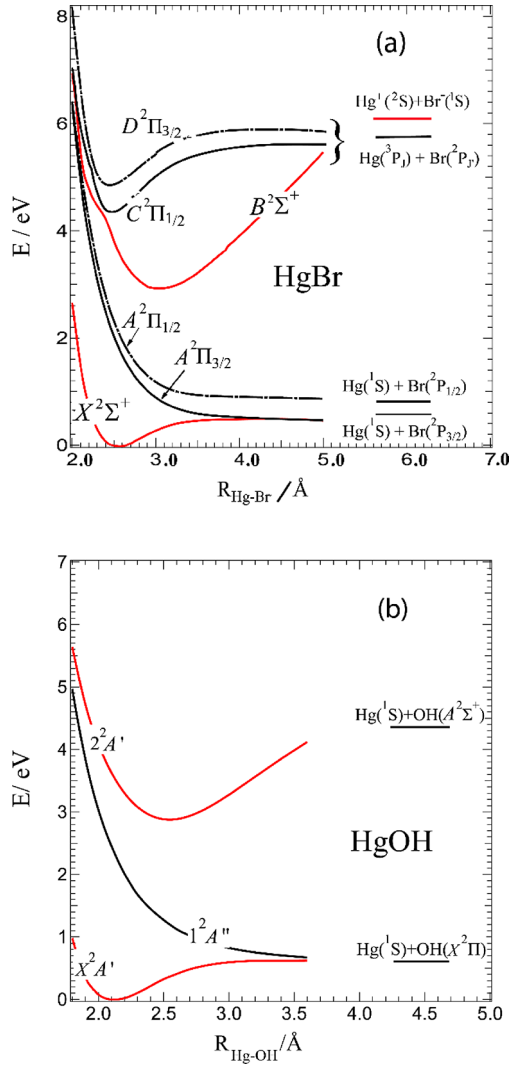

Figure 2. Potential energy curves including SO-effects of the low-lying electronic states of HgBr (a) and HgOH (Hg−OH stretching) (b) as a function of the internuclear distance. SF labels are used here.

charge-transfer component from the halogen atom to Hg (due to electron promotion from the atomic-like p_y orbital of the halogen atom to the σ^{SONO} (see Figure 1)), which neutralizes the charge separation of $X\ ^2\Sigma^+$ ground state and decreases the Coulombic attraction and (ii) the orbital populated (σ^{SONO}) has antibonding character. Light absorption (in the 600−700 nm range, see below) would photodissociate the radicals into Hg(^{1}S) and X($^2P_{1/2,3/2}$) atomic fragments with 100% efficiency.

The first bound excited-state of the monohalide series, $B^2\Sigma^+$ in Figure 2, is an ion-pair[12] fluorescent state which yields the well-known lasing emission.[28−30] The strong Coulombic binding interaction is reflected in the high calculated D_0 values (Table S1 and Figure S3), which only show a modest decrease from 428 in the chlorine radical to 401 kJ·mol^{-1} in the iodine radical, in agreement with experimental observations.

The MS-CASPT2 computed absorption spectra of the mercury monohalides and hydroxyl radical species are presented in Figure 3 (see also Tables S4−S13), for the wavelength range of atmospheric relevance. In addition, numerical cross-section values, with 1 nm resolution, are

DOI: 10.1021/jacs.9b02890
J. Am. Chem. Soc. 2019, 141, 8698−8702

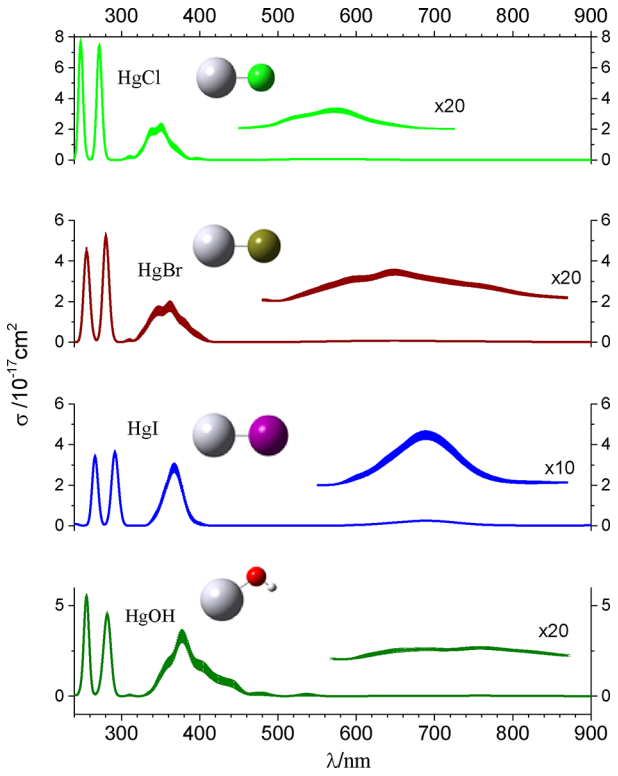

Figure 3. Computed UV−Vis absorption spectra and cross-sections (σ/cm^2) of the HgX (X = Cl, Br, I, OH) radicals studied in this work. The light-colored areas correspond to the uncertainty of the cross-section due to the statistical sampling. Note the different range of σ values for the spectra.

compiled in Table S14. The transition energies computed here in the 200−300 nm UV range (sharp twin peaks, bands C $^2\Pi_{1/2}$ and D $^2\Pi_{3/2}$ reproduce closely (within 1−3%) the experimental values derived from gas-phase emission spectra of the mercury monohalides reported before,[31−33] as well as those from the few available absorption spectra (HgCl, HgI).[34,35] In contrast, a cross-section value of 6×10^{-16} cm^2 for the 279 nm absorption of the HgCl radical estimated previously,[34] is a factor of 10 larger than that computed here. This large value is not consistent with other spectroscopic properties of the radical.

The computed SO splitting of the C $^2\Pi_{1/2}$−D $^2\Pi_{3/2}$ doublet (0.4−0.5 eV) of the monohalides reproduces the experimental value of 3920, 3833, and 3538 cm^{-1} reported for HgCl, HgBr, and HgI, respectively.[35] In the case of HgOH, the broad band observed in the low-resolution absorption spectrum of this radical in aqueous solution[36] shows both, peak location and cross-section, very similar to those presented in Figure 3. Similar experimental data on spectral properties for the HgOH radical in the gas-phase could not be found.

Regarding the 300−700 nm range, experimental data for these radicals are also very scarce. The transient absorption spectra of HgBr in the 240−520 nm range[30,37] shows an intense absorption at ∼350 nm (band B) virtually identical to that computed here, but no data are available on absorption coefficients. Interestingly, these radicals were also detected in the aqueous-phase pulse radiolysis of $HgCl_2$[38] and $HgBr_2$.[39,40] An estimation of the 350 nm absorption cross-section of HgCl and HgBr in aqueous-phase provided values[38,40] of 0.9 and 1.6 $\times 10^{-17}$ cm^2, respectively, consistent with those computed here for the gas-phase species.

In connection with the low-intensity absorption band in the 600−700 nm range (Figure 3), little or no experimental information could be found. A broad absorption continuum centered at ∼600 nm detected in the HgBr transient absorption spectra[41] was assigned to a dissociative transition (band A) predicted theoretically.[42] Similarly, the very weak fluorescence at ∼685 nm was assigned to the $B\ ^2\Sigma^+ - A\ ^2\Pi_{1/2}$ transition in the same radical species,[28] in agreement with the values computed here (Table S8).

From the analysis of the SF deconvolution of the computed SO MS-CASPT2 spectra (Figures S4−S7) and electronic structure (Tables S5−S13), bands C−D, B, and A of the monohalide series can be assigned to the $X^2\Sigma^+ - (C^2\ \Pi_{1/2} - D^2\ \Pi_{3/2})$, $X^2\Sigma^+ - B\ ^2\Sigma^+$, $X^2\Sigma^+ - A^2\ \Pi$ transitions, respectively. These transitions correspond essentially to one-electron promotion from the orbital with the unpaired electron (σ^{SONO}), mainly localized on the 6s Hg atomic orbital (Figure 1), to the $6p_{x/y}$ Hg (band C−D), from the $p_{x/y}$ of the halogen atom to the σ^{SONO} (band B), and from σ bonding orbital to the σ^{SONO} (band A). The doublet at ∼280 nm (bands C and D) and the large bandwidth of the absorption in the dissociative 600−700 nm range (band A) arise from SO coupling effects, which split each of the $^2\ \Pi$ SF transitions into SO pairs, with Ω values of 1/2 and 3/2 (Figure 1; Tables S6, S8, and S10). These sharp C−D doublets may be explained by an excitation more localized on the Hg atom.

For the dissociative band A $^2\Pi$, the calculated SO splitting increases from 0.09 eV (HgCl) to 0.3 eV (HgBr), maintaining similar absorption intensity (Tables S6 and S8), which explains the larger bandwidth of this band in the latter. The splitting is even larger in HgI (0.59 eV, Table S10) and the transition connected with the Ω = 1/2 state becomes much more favored resulting in an intensity increase of the photodissociative band $A^2\Pi$ (Figure 3). See SI for further details.

The absorption cross-sections of HgCl, HgBr, HgI, and HgOH in the 270−800 nm range, excluding the 270−460 nm interval corresponding to non-dissociative transitions to the states B, C, and D, were introduced into a global chemistry-climate model, CAM-Chem,[43,44] to compute the photolysis rate (J/s^{-1}) of each species. The global tropospheric rate of photolysis is 6×10^{-2} s^{-1}, 3×10^{-2} s^{-1}, 2×10^{-2} s^{-1}, and 1×10^{-2} s^{-1} for HgI, HgBr, HgCl, and HgOH, respectively. The competition between thermal-[4] and photoreduction processes of HgBr and its oxidation reactions[45] with the abundant radicals NO_2 and HO_2 (Scheme 1) was determined by calculating the averaged pseudo-first-order rates in the troposphere:

$$HgBr + NO_2 \rightarrow \textit{syn}\text{-BrHgONO} \quad (R1)$$

$$HgBr + HO_2 \rightarrow BrHgOOH \quad (R2)$$

$$HgBr \xrightarrow{\Delta T} Hg + Br \quad (R3)$$

The photolysis of HgBr, globally integrated in the troposphere, is of the same order (10^{-2} s^{-1}) as the pseudo-first-order rates of oxidation by NO_2 R1 and HO_2 R2, and much faster than thermal decomposition R3. Therefore, the photolysis of HgBr will compete with oxidation by NO_2/HO_2 in places with high concentrations of these oxidants. The computed photolysis of HgBr would be faster than the reaction with NO_2/HO_2 in regions free of anthropogenic pollution,

DOI: 10.1021/jacs.9b02890
J. Am. Chem. Soc. 2019, 141, 8698−8702

Scheme 1. The Residence Time of Elemental Mercury Hg(0) in the Atmosphere Is Determined by the Competition between the Rates of Reduction and Oxidation of the HgBr Radical[a]

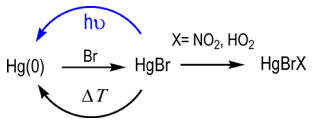

[a]The new HgBr photoreduction process proposed in this study is highlighted in blue.

where NO_2 levels are low, such as the open ocean environments and the mid- to upper-troposphere.

The novel photochemistry of gas-phase Hg(I) radical species has broad implications for atmospheric mercury chemistry. This photoreduction process has been largely overlooked, and our findings suggest that the photolysis of Hg(I) will increase the atmospheric lifetime of mercury, which is key to understanding the global atmospheric mercury cycle. Current atmospheric mercury models, which do not include HgBr photolysis, are clearly underestimating the lifetime of mercury in the atmosphere. Overall, the new findings on the photochemistry of Hg(I) radicals reported in this Communication challenges current kinetic models of atmospheric mercury chemistry.

■ ASSOCIATED CONTENT

Supporting Information

The Supporting Information is available free of charge on the ACS Publications website at DOI: 10.1021/jacs.9b02890.

Computation details, electronic structure tables, thermochemical data and deconvoluted spectra (PDF)

Cross-section data (XLSX)

■ AUTHOR INFORMATION

Corresponding Authors

*a.saiz@csic.es

*Daniel.Roca@uv.es

*frjoseph@sas.upenn.edu

ORCID

Tarek Trabelsi: 0000-0001-6258-7191

Juan Z. Dávalos: 0000-0002-5835-6371

Daniel Roca-Sanjuán: 0000-0001-6495-2770

Joseph S. Francisco: 0000-0002-5461-1486

Notes

The authors declare no competing financial interest.

■ ACKNOWLEDGMENTS

This work was supported by the Consejo Superior de Investigaciones Cientificas (CSIC) of Spain. This study has received funding from the European Research Council Executive Agency under the European Union's Horizon 2020 Research and Innovation programme (Project ERC-2016-COG 726349 CLIMAHAL). This work was supported by the University of Nebraska Holland Computing Center. J.C.-G. acknowledges the Universitat de València for his master scholarship. D.R.-S. is thankful to the Spanish MINECO/FEDER for financial support through Project No. CTQ2017-87054-C2-2-P, the Ramón y Cajal fellowship with ref. RYC-2015-19234, and the Unit of Excellence María de Maetzu MDM-2015-0538. S.P.S. acknowledges the Basque Government for funding through a predoctoral fellowship (PRE 2018 2 0200).

■ REFERENCES

(1) Horowitz, H. M.; Jacob, D. J.; Zhang, Y.; Dibble, T. S.; Slemr, F.; Amos, H. M.; Schmidt, J. A.; Corbitt, E. S.; Marais, E. A.; Sunderland, E. M. A new mechanism for atmospheric mercury redox chemistry: Implications for the global mercury budget. *Atmos. Chem. Phys.* **2017**, *17*, 6353−6371.

(2) Wang, F.; Saiz-Lopez, A.; Mahajan, A. S.; Gómez Martín, J. C.; Armstrong, D.; Lemes, M.; Hay, T.; Prados-Roman, C. Enhanced production of oxidised mercury over the tropical Pacific Ocean: A key missing oxidation pathway. *Atmos. Chem. Phys.* **2014**, *14*, 1323−1335.

(3) Ariya, P. A.; Amyot, M.; Dastoor, A.; Deeds, D.; Feinberg, A.; Kos, G.; Poulain, A.; Ryjkov, A.; Semeniuk, K.; Subir, M.; Toyota, K. Mercury physicochemical and biogeochemical transformation in the atmosphere and at atmospheric interfaces: A review and future directions. *Chem. Rev.* **2015**, *115*, 3760−3802.

(4) Goodsite, M. E.; Plane, J.; Skov, H. A theoretical study of the oxidation of Hg0 to HgBr2 in the troposphere. *Environ. Sci. Technol.* **2004**, *38* (6), 1772−1776.

(5) Holmes, C. D.; Jacob, D. J.; Corbitt, E. S.; Mao, J.; Yang, X.; Talbot, R.; Slemr, F. Global atmospheric model for mercury including oxidation by bromine atoms. *Atmos. Chem. Phys.* **2010**, *10*, 12037−12057.

(6) Saiz-Lopez, A.; Sitkiewicz, S. P.; Roca-Sanjuán, D.; Oliva-Enrich, J. M.; Dávalos, J. Z.; Notario, R.; Jiskra, M.; Xu, Y.; Wang, F.; Thackray, C. P.; Sunderland, E. M.; Jacob, D. J.; Travnikov, O.; Cuevas, C. A.; Acuña, A. U.; Rivero, D.; Plane, J. M. C.; Kinnison, D. E.; Sonke, J. E. Photoreduction of gaseous oxidized mercury changes global atmospheric mercury speciation, transport and deposition. *Nat. Commun.* **2018**, *9* (1), 4796.

(7) Ariya, P. A.; Peterson, K. Chapter 12: Chemical Transformation of gaseous elemental mercury in the atmosphere. In *Dynamics of Mercury Pollution on Regional and Global Scales*; Pirrone, N., Mahaffey, K., Eds.; Springer: New York, 2005.

(8) Si, L.; Ariya, P. A. Reduction of Oxidized Mercury Species by Dicarboxylic Acids (C2−C4): Kinetic and Product Studies. *Environ. Sci. Technol.* **2008**, *42* (14), 5150−5155.

(9) Ohanessian, G.; Brusich, M. J.; Goddard, W. A. Theoretical study of transition-metal hydrides. 5. Hafnium to mercury (HfH+ through HgH+), barium and lanthanum (BaH+ and LaH+). *J. Am. Chem. Soc.* **1990**, *112* (20), 7179−7189.

(10) Siegbahn, P. E. M.; Svensson, M.; Crabtree, R. H. A Theoretical Study of Mercury Photosensitized Reactions. *J. Am. Chem. Soc.* **1995**, *117* (25), 6758−6765.

(11) Duzy, C.; Hyman, H. A. Radiative lifetimes for the B→X transition in HgCl, HgBr, and HgI. *Chem. Phys. Lett.* **1977**, *52* (2), 345−348.

(12) Wadt, W. R. The electronic structure of HgCl and HgBr. *Appl. Phys. Lett.* **1979**, *34* (10), 658−660.

(13) Julienne, P. S.; Konowalow, D. D.; Krauss, M.; Rosenkrantz, M. E.; Stevens, W. J. Photodissociation of HgCl. *Appl. Phys. Lett.* **1980**, *36* (2), 132−134.

(14) Krauss, M.; Stevens, W. J. Photodissociation of HgBr, XΣ1/2. *Appl. Phys. Lett.* **1981**, *39* (9), 686−688.

(15) Tossell, J. A. Calculation of the Energetics for Oxidation of Gas-Phase Elemental Hg by Br and BrO. *J. Phys. Chem. A* **2003**, *107* (39), 7804−7808.

(16) Knowles, P. J.; Werner, H.-J. An efficient second-order MC SCF method for long configuration expansions. *Chem. Phys. Lett.* **1985**, *115* (3), 259−267.

(17) Werner, H. J.; Knowles, P. J. A second order multiconfiguration SCF procedure with optimum convergence. *J. Chem. Phys.* **1985**, *82* (11), 5053−5063.

DOI: 10.1021/jacs.9b02890
J. Am. Chem. Soc. 2019, 141, 8698−8702

(18) Werner, H. J.; Knowles, P. J. An efficient internally contracted multiconfiguration−reference configuration interaction method. *J. Chem. Phys.* **1988**, *89* (9), 5803−5814.
(19) Knowles, P. J.; Werner, H.-J. An efficient method for the evaluation of coupling coefficients in configuration interaction calculations. *Chem. Phys. Lett.* **1988**, *145* (6), 514−522.
(20) Langhoff, S. R.; Davidson, E. R. Configuration interaction calculations on the nitrogen molecule. *Int. J. Quantum Chem.* **1974**, *8* (1), 61−72.
(21) Finley, J.; Malmqvist, P.-Å.; Roos, B. O.; Serrano-Andrés, L. The multi-state CASPT2 method. *Chem. Phys. Lett.* **1998**, *288* (2), 299−306.
(22) Andersson, K.; Malmqvist, P. A.; Roos, B. O.; Sadlej, A. J.; Wolinski, K. Second-order perturbation theory with a CASSCF reference function. *J. Phys. Chem.* **1990**, *94* (14), 5483−5488.
(23) Andersson, K.; Malmqvist, P. Å.; Roos, B. O. Second-order perturbation theory with a complete active space self-consistent field reference function. *J. Chem. Phys.* **1992**, *96* (2), 1218−1226.
(24) Roca-Sanjuán, D.; Aquilante, F.; Lindh, R. Multiconfiguration second-order perturbation theory approach to strong electron correlation in chemistry and photochemistry. *Wiley Interdisciplinary Reviews: Computational Molecular Science* **2012**, *2* (4), 585−603.
(25) Aquilante, F.; Autschbach, J.; Carlson, R. K.; Chibotaru, L. F.; Delcey, M. G.; De Vico, L.; Ferré, N.; Frutos, L. M.; Gagliardi, L.; Garavelli, M. Molcas 8: New capabilities for multiconfigurational quantum chemical calculations across the periodic table. *J. Comput. Chem.* **2016**, *37* (5), 506−541.
(26) Sitkiewicz, S. P.; Oliva, J. M.; Dávalos, J. Z.; Notario, R.; Saiz-Lopez, A.; Alcoba, D. R.; Oña, O. B.; Roca-Sanjuán, D. Ab initio quantum−chemical computations of the electronic states in HgBr2 and IBr: Molecules of interest on the Earth's atmosphere. *J. Chem. Phys.* **2016**, *145* (24), 244304.
(27) Sitkiewicz, S. P.; Rivero, D.; Oliva-Enrich, J. M.; Saiz-Lopez, A.; Roca-Sanjuán, D. Ab initio quantum-chemical computations of the absorption cross-sections of HgX2 and HgXY (X, Y = Cl, Br, and I): molecules of interest in the Earth's atmosphere. *Phys. Chem. Chem. Phys.* **2019**, *21* (1), 455−467.
(28) Tellinghuisen, J.; Ashmore, J. G. The B→X transition in 200Hg 79Br. *Appl. Phys. Lett.* **1982**, *40* (10), 867−869.
(29) Tellinghuisen, J.; Ashmore, J. G. Mixed representations for diatomic spectroscopic data: Application to HgBr. *Chem. Phys. Lett.* **1983**, *102* (1), 10−16.
(30) Greene, D. P.; Killeen, K. P.; Eden, J. G. Excitation of the HgBr B2Σ1/2+←X2Σ1/2+ band in the ultraviolet. *J. Opt. Soc. Am. B* **1986**, *3* (10), 1282−1287.
(31) Wieland, K. *Helv. Phys. Acta* **1929**, *2*, 46.
(32) Howell, H. G. The ultra-violet spectra and electron configuration of HgF and related halide molecules. *Proc. R. Soc. (London)* **1943**, *182*, 95.
(33) Cornell, S. D. Ultraviolet Band Spectra of HgCl, CdCl, and ZnCl. *Phys. Rev.* **1938**, *54* (5), 341−346.
(34) Horne, D. G.; Gosavi, R.; Strausz, O. P. Reactions of Metal Atoms. I. The Combination of Mercury and Chlorine Atoms and the Dimerization of HgCl. *J. Chem. Phys.* **1968**, *48* (10), 4758−4764.
(35) Greig, G.; Gunning, H. E.; Strausz, O. P. Reactions of Metal Atoms. III. The Combination of Mercury and Iodine Atoms and the Spectrum of HgI. *J. Chem. Phys.* **1970**, *52* (9), 4569−4571.
(36) Fujita, S.; Horii, H.; Mori, T.; Taniguchi, S. Pulse radiolysis of mercuric oxide in neutral aqueous solutions. *J. Phys. Chem.* **1975**, *79* (10), 960−964.
(37) Greene, D. P.; Killeen, K. P.; Eden, J. G. X2Σ→B2Σ absorption band of HgBr: Optically pumped 502-nm laser. *Appl. Phys. Lett.* **1986**, *48* (18), 1175−1177.
(38) Nazhat, N. B.; Asmus, K. D. Reduction of mercuric chloride by hydrated electrons and reducing radicals in aqueous solutions. Formation and reactions of mercury chloride (HgCl). *J. Phys. Chem.* **1973**, *77* (5), 614−620.
(39) Fujita, S.-i.; Horii, H.; Mori, T.; Taniguchi, S. Pulse Radiolysis of $HgBr_2$ in Aqueous Solutions. *Bull. Chem. Soc. Jpn.* **1976**, *49* (5), 1250−1253.
(40) Jungbluth, H.; Beyrich, J.; Asmus, K. D. Reduction of mercuric halides and pseudohalides in aqueous solution. Formation and some physicochemical properties of mercury(I) chloride, mercury(I) bromide, mercury(I) iodide, mercury(I) thiocyanate, and mercury(I) cyanide radical molecules. *J. Phys. Chem.* **1976**, *80* (10), 1049−1053.
(41) Baker, H. J.; Seddon, N. Transient absorption processes in a mercury bromide laser discharge. *J. Phys. D: Appl. Phys.* **1988**, *21* (9), 1347−1351.
(42) Lapatovich, W. P.; Gibbs, G. R.; Proud, J. M. Bound-free emission in HgBr. *Appl. Phys. Lett.* **1982**, *41* (9), 786−788.
(43) Ordóñez, C.; Lamarque, J. F.; Tilmes, S.; Kinnison, D. E.; Atlas, E. L.; Blake, D. R.; Sousa Santos, G.; Brasseur, G.; Saiz-Lopez, A. Bromine and iodine chemistry in a global chemistry-climate model: description and evaluation of very short-lived oceanic sources. *Atmos. Chem. Phys.* **2012**, *12* (3), 1423−1447.
(44) Saiz-Lopez, A.; Lamarque, J. F.; Kinnison, D. E.; Tilmes, S.; Ordóñez, C.; Orlando, J. J.; Conley, A. J.; Plane, J. M. C.; Mahajan, A. S.; Sousa Santos, G.; Atlas, E. L.; Blake, D. R.; Sander, S. P.; Schauffler, S.; Thompson, A. M.; Brasseur, G. Estimating the climate significance of halogen-driven ozone loss in the tropical marine troposphere. *Atmos. Chem. Phys.* **2012**, *12* (9), 3939−3949.
(45) Jiao, Y.; Dibble, T. S. First kinetic study of the atmospherically important reactions BrHġ + NO_2 and BrHġ + HOO. *Phys. Chem. Chem. Phys.* **2017**, *19* (3), 1826−1838.

DOI: 10.1021/jacs.9b02890
J. Am. Chem. Soc. 2019, 141, 8698−8702